



A Total Variation Diminishing Hopmoc Scheme for Numerical Time Integration of Evolutionary Differential Equations

Diego N. Brandão¹ , Sanderson L. Gonzaga de Oliveira²(✉) ,
Mauricio Kischinhevsky³ , Carla Osthoff⁴ , and Frederico Cabral⁴ 

¹ CEFET-RJ, Rio de Janeiro, RJ, Brazil
diego.brandao@eic.cefet-rj.br

² Universidade Federal de Lavras, Lavras, MG, Brazil
sanderson@dcc.ufla.br

³ Universidade Federal Fluminense, Niterói, RJ, Brazil
kisch@ic.uff.br

⁴ Laboratório Nacional de Computação Científica (LNCC), Petrópolis, RJ, Brazil
{osthoff,fcabral}@lncc.br

Abstract. This paper concentrates on a total variation diminishing Hopmoc scheme for numerical time integration of evolutionary differential equations. The Hopmoc method for numerical integration of parabolic partial differential equations with convective dominance is based on the concept of spatially decomposed meshes used in the Hopscotch method. In addition, the Hopmoc method uses the concept of integration along characteristic lines in a Semi-Lagrangian scheme based on the Modified Method of Characteristics. This work employs Total Variation Diminishing schemes in order to increase accuracy of the Hopmoc method. Thus, this paper shows that the Hopmoc method in conjunction with a Total Variation Diminishing scheme provides effective improvements over the original Hopmoc method.

Keywords: Higher-order schemes · Total Variation Diminishing Flux limiters · Hopscotch method · Advection-diffusion equation Modified Method of Characteristics

1 Introduction

The numerical solution of advection–diffusion transport arises from several relevant scientific and engineering applications, including problems in physics and chemistry. Important examples of its use include the transport of contaminants in air, ground water, rivers, and lagoons, oil reservoir flow, aerodynamics, astrophysics, biomedical applications, in the modeling of semiconductors, geophysical flows, such as meteorology and oceanography [1]. In reactive or environment fluid flow problems, contaminant or chemical species are mainly transported by the fluid in which it is dissolved. Specifically in computational hydraulics and fluid

dynamics problems, the advection–diffusion equation can be used to represent quantities such as mass, heat, energy, vorticity, etc. [2]. Thus, the modeling of transport processes is studied in a wide range of fields. Therefore, this is a key topic in numerical mathematics [3].

The Hopmoc method was proposed to solve parabolic problems with convective dominance in parallel architectures [4, 5]. This method addresses the entire process of parallelization by devising a spatial decoupling that allows message-passing minimization.

The Hopscotch method [6–10] is a general-purpose approach for the solution of second-order parabolic and elliptic partial differential equations. The Hopmoc method [4, 5] is based on Hopscotch concepts in the sense that the set of unknowns is decoupled into two subsets. These subsets are calculated alternately in explicit and implicit semi-steps so that the approach does not involve solving any linear system. The semi-steps are solved along characteristic lines in a Semi-Lagrangian approach following concepts of the Modified Method of Characteristics [11]. The time derivative and the advection term are integrated as a direction derivative, i.e. time steps are calculated in the flow direction along characteristics of the velocity field of the fluid. Specifically, the Hopmoc method uses a strategy based on tracking values along characteristic lines during time stepping. Furthermore, it is an Eulerian-Lagrangian localized adjoint method (ELLAM [12]) since the domain is completely discretized along characteristic lines. In short, an ELLAM-like method provides the accuracy and efficiency of an Eulerian-Lagrangian approach, preserves mass quantity, and systematically handles any sort of boundary condition [13]. In addition, the Hopmoc method is a direct method in the sense that the cost per time step is known *a priori* [1]. Another advantage of the Hopmoc method is that its processing time is linear in the number of unknowns per time step [14].

Discretization of the advective term in transport equations is frequently a difficult task. To avoid abrupt numerical oscillations in the solution, Harten [15] introduced the concepts of Total Variation Diminishing (TVD) techniques and flux limiter. In short, these techniques provide monotonicity-preserving properties of stable higher-order accurate solutions of advection–diffusion problems. Total Variation Diminishing techniques have been successfully employed alongside numerical methods, where recent examples are the publications of Bartels [16] and Fernandes et al. [17].

This paper implements a Total Variation Diminishing technique along with the Hopmoc method. More specifically, this work shows how to combine a total variation diminishing scheme for numerical time integration of parabolic equations with convective dominance when using the Hopmoc method.

The remainder of this paper is divided as follows. Section 2 provides a brief background on the original Hopmoc scheme, which we modify and improve in this paper. Section 3 describes the Total Variation Diminishing scheme employed and the different flux limiters used in this work. Section 4 shows the numerical results. Specifically, this section shows the efficiency of the new scheme over the

original Hopmoc method in terms of numerical errors. Section 5 addresses the final remarks and a description of future works.

2 The Hopmoc Method

For clarity, we describe below the Hopmoc method in details (see [4, 5]). Consider the one-dimensional advection–diffusion equation in the form

$$u_t + vu_x = du_{xx}, \quad (1)$$

comprised of appropriate initial and boundary conditions, where v is a constant positive velocity, d is a positive constant of diffusivity, and $0 \leq x \leq 1$. Even though in Eq. (1) u_t refers to the time derivative and not u evaluated at a discrete time step t , we abuse the notation and now use t to represent a discrete time step in the range $0 \leq t \leq T$, for T time steps. Then, $\Delta t = u^{t+1} - u^t$ ($\delta t = \frac{\Delta t}{2} = u^{t+\frac{1}{2}} - u^t$) represents a time (semi-) step when considering a typical finite-difference discretization for Eq. (1). Specifically, this work uses a three-point finite-difference scheme for the discretization of diffusive terms.

Figure 1 represents the Hopmoc method for a one-dimensional problem. This figure shows that the characteristic line allows to obtain $\bar{u}(\bar{x}_i^{t+\frac{1}{2}})$ and $\bar{\bar{u}}(\bar{\bar{x}}_i^t)$ in the previous two time semi-steps, for $\bar{x}_i^{t+\frac{1}{2}} = x_i - v \cdot \delta t$ and $\bar{\bar{x}}_i^t = x_i - 2v \cdot \delta t$, respectively. As described below, an interpolation calculates the variable value $\bar{\bar{u}}(\bar{\bar{x}}_i^t)$ [18]. For clarity, a variable in a previous time [semi-] step is represented as $\bar{\bar{u}}_i^t = u(\bar{\bar{x}}_i^t) [\bar{\bar{u}}_i^{t+\frac{1}{2}} = u(\bar{\bar{x}}_i^{t+\frac{1}{2}})]$ in the foot of the characteristic line originated at $\bar{\bar{x}}_i^t [\bar{x}_i^{t+\frac{1}{2}}]$. The Hopmoc method performs this strategy along characteristic lines in a Semi-Lagrangian scheme based on the Modified Method of Characteristics [11]. Thus, $\bar{\bar{u}}_i^t [\bar{\bar{u}}_i^{t+1}]$ is a numerical approximation of u in $(x_i, u^t) [(x_i, u^{t+1})]$. In addition, a uniform spatial discretization $\Delta x = x_{i+1} - x_i$ is used [18]. Thereby, the Hopmoc method uses variable values $\bar{\bar{u}}_i^t(\bar{\bar{x}}_i^{t+\frac{1}{2}})$ to calculate $\bar{\bar{u}}_i^{t+\frac{1}{2}}(u_i^{t+1})$ in its first (second) time semi-step.

The set of grid points is divided into two subsets during the implementation of the integration step (see Fig. 1). Then, two distinct updates are alternately performed, one explicit and one implicit, on each variable in the course of the iterative process. Each update demands an integration semi step. Similar to the Hopscotch method, this approach avoids the use of a linear system solver to calculate the unknowns, as mentioned.

The Hopmoc method employs the finite-difference operator

$$L_h(u_i^t) = d \frac{u_{i-1}^t - 2u_i^t + u_{i+1}^t}{\Delta x^2} \quad (2)$$

so that both consecutive time semi-steps can be written as $\bar{\bar{u}}_i^{t+\frac{1}{2}} = \bar{\bar{u}}_i^t + \delta t \left(\theta_i^t L_h \bar{\bar{u}}_i^t + \theta_i^{t+1} L_h \bar{\bar{u}}_i^{t+\frac{1}{2}} \right)$ or $u_i^{t+1} = \bar{\bar{u}}_i^{t+\frac{1}{2}} + \delta t \left(\theta_i^t L_h \bar{\bar{u}}_i^{t+\frac{1}{2}} + \theta_i^{t+1} L_h u_i^{t+1} \right)$, for

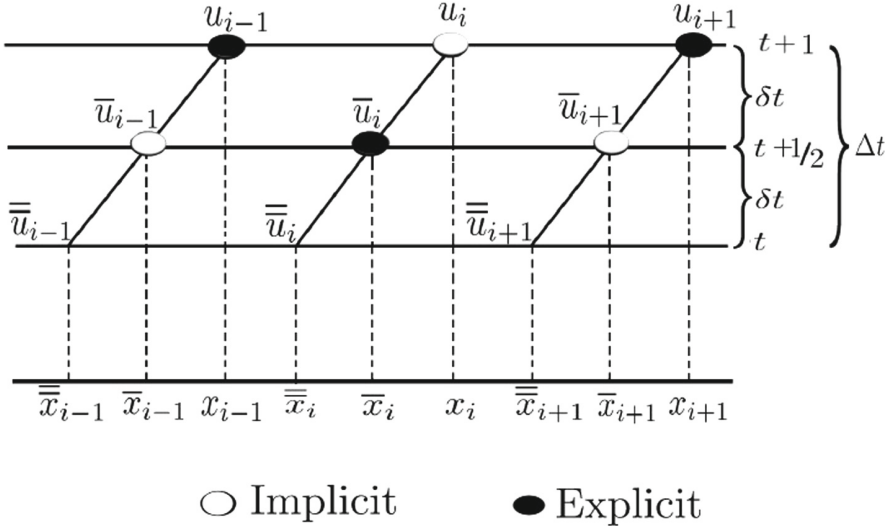


Fig. 1. Variable values $\bar{\bar{u}}_i^t$ are used to calculate $\bar{u}_i^{t+\frac{1}{2}}$ in a first time semi-step and subsequently the variable values $\bar{u}_i^{t+\frac{1}{2}}$ are used to calculate u_i^t in the second time semi-step in the Hopmoc method

$\theta_i^t = 1$ ($= 0$) if $t + i$ is even (odd). In particular, Oliveira et al. [18] presented the convergence analysis of the Hopmoc method for an advection–diffusion equation.

The discretization of the advective term demands to calculate the values of the concentration at midpoints of the sides of each grid interval. Thus, this work employs a flux limiter to obtain these values.

As mentioned, the Hopmoc method employs in each first step a linear interpolation to obtain the initial estimative of the function value in the foot of the characteristic line. Consider a complete Hopmoc step in order to calculate u_i^{t+1} when t is even: $\bar{u}_i^{t+\frac{1}{2}}$ are updated using $\bar{\bar{u}}_i^t$ in the first time semi-step, i.e., $\bar{\bar{u}}_i^t$ are obtained by a linear interpolation using values u_i^t from the previous time step, since these values are already known from the previous time step. When using a linear interpolation, one obtains $\bar{\bar{u}}_i^t = u_{i-q-1}^t + \frac{u_{i-q}^t - u_{i-q-1}^t}{x_{i-q} - x_{i-q-1}}(\bar{\bar{x}}_i - x_{i-q-1})$, where $q = \lfloor \frac{\Delta t}{\Delta x} \rfloor$ is the number of spatial intervals to be jumped to find $\bar{\bar{x}}_i = x_i - v\Delta t$, so that (x_{i-q-1}, x_{i-q}) is the interpolation interval sought. Consequently, $\bar{\bar{x}}_i \in (x_{i-q-1}, x_{i-q})$. Therefore, the linear interpolation is

$$\bar{\bar{u}}_i^t = \frac{(x_{i-q} - \bar{\bar{x}}_i) u_{i-q-1}^t + (\bar{\bar{x}}_i - x_{i-q-1}) u_{i-q}^t}{x_{i-q} - x_{i-q-1}}. \quad (3)$$

Substituting $\Delta x = x_{i-q} - x_{i-q-1}$ and $\bar{x}_i = x_i - \Delta t$ for $v = 1$ in Eq. (3) yields

$$\bar{u}_i^t = \frac{\overbrace{(x_{i-q} - x_i + \Delta t)u_{i-q-1}^t}^{-q\Delta x} + \overbrace{(x_i - x_{i-q-1} - \Delta t)u_{i-q}^t}^{(q+1)\Delta x}}{\Delta x}. \quad (4)$$

Each nodal point in the spatial discretization is given by $x_i = i \cdot \Delta x$, for $i = 0, 1, \dots, N$ in N spatial intervals. Therefore, substituting $-q\Delta x = x_{i-q} - x_i$ and $(q+1)\Delta x = x_i - x_{i-q-1}$ in Eq. (4) yields

$$\bar{u}_i^t = \left(\frac{\Delta t}{\Delta x} - q \right) (u_{i-q-1}^t - u_{i-q}^t) + u_{i-q}^t. \quad (5)$$

The origin of the error in Eq. (5) occurs as described below [18].

- Error increases if $\Delta t < \Delta x$. In this case, $q = 0$ is obtained and the interpolation step contains a nodal point x_i , i.e., $\bar{x}_i \in (x_{i-1}, x_i)$. Rewriting Eq. (5) provides $\bar{u}_i^t = \left(\frac{\Delta t}{\Delta x} \right) u_{i-1}^t + \left(1 - \frac{\Delta t}{\Delta x} \right) u_i^t$. When Δt decreases, the foot of the characteristic line approximates x_i . Thus, the factor $1 - \frac{\Delta t}{\Delta x}$ increases. This means that if a higher weight is given to the value u_i^t , the error gradually increases. Nevertheless, u_{i-1}^t represents upstream information. Since $\bar{x}_i = x_i - \Delta t$, the foot of the characteristic line approximates x_i when Δt decreases. The expected result is to reduce the maximum error. However, if $\Delta t < \Delta x$, then the error increases when Δt decreases because of the use of a linear interpolation.
- Error oscillates if $\Delta t \geq \Delta x$. The errors of the scheme present oscillations with respect to $\frac{\Delta t}{\Delta x}$. If this quotient is an integer number, the error is smaller; otherwise, it is either increased or reduced, and the analysis is divided into the two cases described below.
 1. Δt is multiple of Δx and $\frac{\Delta t}{\Delta x} - q = 0$ in Eq. (5). This means that the foot of the characteristic line \bar{x}_i coincides with a nodal point. Thus, each \bar{u}_i^t is directly updated from the value u_{i-q}^t , which in turn was updated after a Hopmoc step in the second time semi-step t , i.e. $\bar{u}_i^t = u_{i-q}^t$. Therefore, the values $\bar{u}_i^{t+\frac{1}{2}}$ and u_i^{t+1} are updated without any error originated from a linear interpolation. More precisely, a linear interpolation is not carried out if the foot of the characteristic line is a nodal point. For this reason, the error is considerably reduced if compared with simulations where a linear interpolation occurs. This can be observed in Table 1, when considering Eq. (2). In particular, this table shows inherent truncation errors in simulations with the Hopmoc method even without using linear interpolation because the use of large time steps (see rows with $\frac{\Delta t}{\Delta x} \geq 4$ in Table 1).
 2. Δt is not multiple of Δx . Considering Eq. (5), the interpolation of the values \bar{u}_i^t are calculated as $\bar{u}_i^t = \left(\frac{\Delta t}{\Delta x} - q \right) u_{i-q-1}^t + \left[1 - \left(\frac{\Delta t}{\Delta x} - q \right) \right] u_{i-q}^t$.

Table 1. Maximum errors when setting $\Delta x = 0.001$ and applying the Hopmoc method with and without (w/o) using linear interpolation (int.)

Δt	$\frac{\Delta t}{\Delta x}$	$d = 0.002$		$d = 0.001$		$d = 0.000\bar{6}$	
		int.	w/o int.	int.	w/o int.	int.	w/o int.
$2.00 \cdot 10^{-4}$	0.2000	1.5138	0.0	3.1551	0.0	4.5060	0.0
$2.50 \cdot 10^{-4}$	0.2500	1.4929	0.0	2.9897	0.0	4.2807	0.0
$31.25 \cdot 10^{-5}$	0.3125	1.3215	0.0	2.7781	0.0	3.9905	0.0
$4.00 \cdot 10^{-4}$	0.4000	1.1678	0.0	2.4721	0.0	3.5678	0.0
$5.00 \cdot 10^{-4}$	0.5000	0.9876	0.0	2.1075	0.0	3.0590	0.0
$6.25 \cdot 10^{-4}$	0.6250	0.7549	0.0	1.6279	0.0	2.3807	0.0
$8.00 \cdot 10^{-4}$	0.8000	0.4141	0.0	0.9066	0.0	1.3410	0.0
$1.00 \cdot 10^{-3}$	1.0000	0.0012	0.0	0.0008	0.0	0.0001	0.0
$1.25 \cdot 10^{-3}$	1.2500	0.3154	0.0	0.6906	0.0	1.0236	0.0
$156.25 \cdot 10^{-5}$	1.5625	0.3375	0.0	0.7272	0.0	1.0742	0.0
$1.00 \cdot 10^{-3}$	4.0000	0.1695	0.0003	0.0803	0.0003	0.0457	0.0002
$1.00 \cdot 10^{-2}$	10.0000	1.0749	0.0021	0.5188	0.0019	0.3011	0.0015

3 A Total Variation Diminishing Scheme

Consider the advection part of Eq. (1), i.e.

$$u_t + v \cdot u_x = 0, \quad (6)$$

for the case when u is constant and positive. In addition, consider u_i^t as a discrete approximation to u in a grid point at time step t . Harten [15] explained that a weak solution of a scalar initial value problem has a monotonicity property as a function of t , i.e. no new local extrema in the solution spatial domain may be created; and the value of a local minimum (maximum) is non-decreasing (non-increasing).

Consider the total variation (TV) at time step t defined as $TV^t = \sum_i |u_{i+1}^t - u_i^t|$. It follows from this monotonicity property that the total variation is non-increasing in t , i.e. a scheme is Total Variation Diminishing if it guarantees that $TV^{t+1} \leq TV^t$.

The Total Variation Diminishing property should be evaluated globally in a solution of an advection scheme. The Total Variation Diminishing property guarantees that the total variation of the solution will not increase as the solution evolves in time. Harten [15] demonstrated that an initially monotonic profile u_i^t remains monotonic after advection by a Total Variation Diminishing scheme. Consider the Eq. (6) rewritten in the form

$$u_i^{t+1} = u_i^t - C_{i-\frac{1}{2}} (u_i^t - u_{i-1}^t) + D_{i+\frac{1}{2}} (u_{i+1}^t - u_i^t), \quad (7)$$

where values represented in C and D may depend on unknowns u_i^t as well as on u . Harten [15] showed that the conditions

$$0 \leq C_{i+\frac{1}{2}}, 0 \leq D_{i+\frac{1}{2}}, C_{i+\frac{1}{2}} + D_{i+\frac{1}{2}} \leq 1, \quad (8)$$

for all i , are sufficient to ensure that the scheme is Total Variation Diminishing. Thus, when building a Total Variation Diminishing scheme, one considers a basic advection scheme, rewrites it in the form of Eq. (7), and then modifies it in a manner that satisfies the conditions in (8). To exemplify this approach, we consider a discretization in the form

$$u_i^{t+1} = u_i^t - c \cdot \left(\hat{u}_{i+\frac{1}{2}} - \hat{u}_{i-\frac{1}{2}} \right), \quad (9)$$

where $c = v \frac{\Delta t}{\Delta x}$ is the Courant number and values represented in \hat{u} are mixing ratios at the grid box edges. To illustrate the definition of \hat{u} , we use the Lax–Wendroff scheme $\hat{u}_{i+\frac{1}{2}} = u_i^t + \frac{1-c}{2} (u_{i+1}^t - u_i^t)$ [19].

The Total Variation Diminishing scheme is built when a factor ϕ is introduced, called *flux limiter*,

$$\hat{u}_{i+\frac{1}{2}} = u_i^t + \phi_i \frac{1-c}{2} (u_{i+1}^t - u_i^t). \quad (10)$$

In general, ϕ depends on u and then it may change with respect to position and time. Two particular cases are the Lax–Wendroff scheme (when $\phi_i = 1$) and the classical upwind scheme (when $\phi_i = 0$) [20]. Thus, Eqs. (9) and (10) can be combined as $u_{i+1} = u_i^t - c(u_i^t - u_{i-1}^t) \left[1 - \frac{1-c}{2} \phi_{i-1} + \frac{1-c}{2} \cdot \frac{\phi_i}{r} \right]$, where $r = \frac{u_i^t - u_{i-1}^t}{u_{i+1}^t - u_i^t}$. Observing that $c < 1$ and to guarantee that this scheme is Total Variation Diminishing, the conditions $0 \leq \phi_i \leq \frac{2}{1-c}$ and $0 \leq \frac{\phi_i}{r_i} \leq \frac{2}{c}$ for all i must be applied. To avoid the CFL condition, those conditions can be rewritten as $0 \leq \phi_i \leq 2$ and $0 \leq \frac{\phi_i}{r_i} \leq 2$, for all i . These conditions are satisfied by several flux limiters [3, 19, 21], and the same approach can be used in conjunction with any high-order basic advection scheme [19].

Flux limiters define the advection scheme based on a ratio of local gradients in the solution field [21, 22]. To be used in conjunction with the Hopmoc method, this work compares five flux–limiter formulations based on [23] because the spatial terms are completely separated from the time discretization in their formulations.

- MinMod is a symmetric piecewise-linear scheme proposed by Roe and Baines [23]. It represents the simple expedient of centered gradients from extrema [21]: $\phi(r) = \max[0, \min(r, 1)]$.
- Superbee is a symmetric piecewise-linear scheme proposed by Roe [24]: $\phi(r) = \max[0, \min(2r, \max(r, 1), 2)]$. This scheme is a highly compressive transfer function. It was developed to achieve the best possible resolution in discontinuities.

- Van Leer is a symmetric non-linear scheme proposed by Van Leer [25] defined as $\phi(r) = \max[0, \min(\theta r, 1), \min(\theta, r)]$ with $1 \leq \theta \leq 2$, so that $\phi(r) = \frac{r+|r|}{1+|r|}$. It is based on consecutive gradients and is a particular-case TVD scheme that includes extrema both in the upper and lower boundaries.
- Monotonized Central (MC) is a symmetric scheme proposed also by Van Leer [25]. It compares the central difference slope of a centered slope method with twice the one-sided slope to a side: $\phi(r) = \max[0, \min(2r, \frac{1+r}{2}, 2)]$.
- Koren's scheme [26] consists of a non-linear symmetric technique. A version of this scheme applied to variable grid size was presented by Holstad [3]: $\phi(r) = \max[0, \min(4r, \frac{2}{3}r + \frac{1}{3}, 2)]$.

The use of a TVD technique does not change the complexity of the 1-D Hopmoc method. This occurs because, similar to the MMOC, the loop that calculates a TVD technique takes $O(n)$ time.

4 Numerical Results and Analysis

Consider the one-dimensional advection–diffusion Eq. (1) with velocity $v = 1.0$ and diffusion coefficient $d = \frac{2}{Re}$. Thus, Eq. (1) is rewritten as

$$u_t + u_x = \frac{2}{Re} u_{xx}. \quad (11)$$

The analytical solution to (11) in a smooth domain is

$$U(x, t) = \frac{\exp\left[-\frac{(x-x_o-t)^2}{2 \cdot \phi(t)}\right]}{\sqrt{\phi}}, \quad (12)$$

where $\phi(t) = \phi_o \left[1 + \frac{4t}{Re\phi_o}\right]$, x_o is the initial center location of the pulse, $Re = \frac{\rho \cdot L \cdot v}{\mu}$ is the Reynolds number, ρ , L , v , and μ represent density, size of the draining, velocity, and viscosity of the fluid, respectively, and ϕ_o is the Gaussian pulse amplitude. A Gaussian pulse with amplitude 0.0004, whose initial center location is 0.2, is simulated in our numerical experiments. The initial and boundary conditions simulate the analytical value $U(x, t)$ given by Eq. (12), for $0 \leq x \leq 1$ and $0 \leq t \leq T$.

The workstation used in the execution of the simulations contains an Intel® Core™ i5 with 4 GB of main memory, OS X version 10.10.1 (Intel; Santa Clara, CA, United States). The maximum error was defined as $\max|U(x, t) - u_t^i|$.

As described, Table 1 shows the results of the original Hopmoc method when using interpolation. These results were compared with the results obtained when using a Total Variation Diminishing scheme to determine the foot of the characteristic line in the Hopmoc method. We will refer this approach as TVD–Hopmoc method.

Table 2 shows the maximum errors when establishing $\Delta x = 0.001$ and Reynolds number (Re) as 1000 and, consequently, $d = 0.002$. This table shows the

Table 2. Maximum errors from the TVD-Hopmoc method when setting $\Delta x = 0.001$ and Reynolds number $Re = 1000$ compared with maximum errors in simulations using the original Hopmoc method. The symbol \dagger indicates that the convergence was not achieved

Δt	$\frac{\Delta t}{\Delta x}$	Hopmoc		TVD-Hopmoc				
		w/o int.	int.	Van Leer	MinMod	Superbee	MC	Koren
$2.00 \cdot 10^{-4}$	0.20	0.0000	1.5138	0.0048	0.0310	0.0306	0.0048	0.0124
$2.50 \cdot 10^{-4}$	0.25	0.0000	1.4929	0.0038	0.0296	0.0284	0.0038	0.0109
$31.25 \cdot 10^{-5}$	0.31	0.0000	1.3215	0.0027	0.0274	0.0255	0.0026	0.0092
$4.00 \cdot 10^{-4}$	0.40	0.0000	1.1678	0.0023	0.0235	0.0215	0.0014	0.0071
$5.00 \cdot 10^{-4}$	0.50	0.0000	0.9876	0.0028	0.0213	0.0163	0.0019	0.0050
$6.25 \cdot 10^{-4}$	0.63	0.0000	0.7549	0.0031	0.0170	0.0104	0.0023	0.0031
$8.00 \cdot 10^{-4}$	0.80	0.0000	0.4141	0.0031	0.0089	0.0028	0.0028	0.0022
$1.00 \cdot 10^{-3}$	1.00	0.0000	0.0012	\dagger				
$1.25 \cdot 10^{-3}$	1.25	0.0000	0.3154					
$156.25 \cdot 10^{-5}$	1.56	0.0000	0.3375					
$4.00 \cdot 10^{-3}$	4.00	0.0003	0.1695					
$1.00 \cdot 10^{-2}$	10.00	0.0021	0.0749					

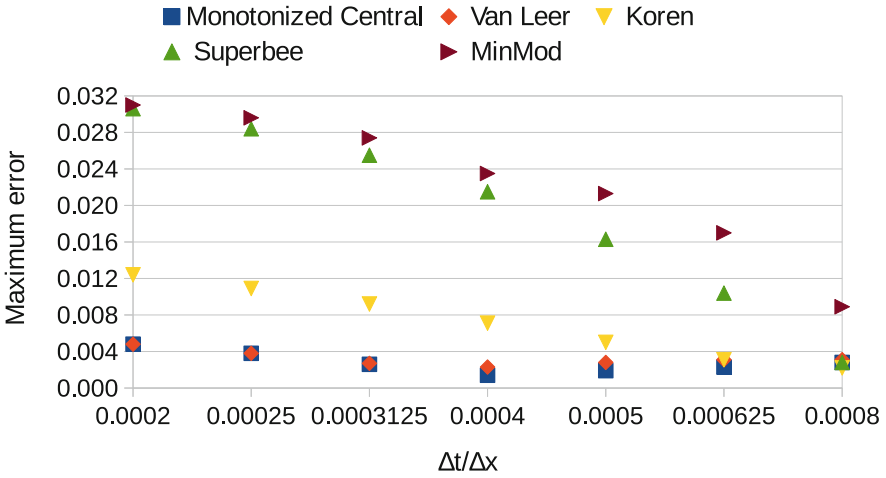


Fig. 2. Maximum errors when setting $\Delta x = 0.001$ and Reynolds number (Re) established as 1000 in simulations employing the TVD-Hopmoc method alongside five flux-limiter formulations

maximum errors of the original Hopmoc method with and without (w/o) using linear interpolation (int.). This table and Fig. 2 show that the Monotonized Central scheme reached the best results when used along with the TVD-Hopmoc method.

Table 3 shows the results when setting the Reynolds number as 2000 ($d = 0.001$) and 3000. Tables 2 and 3 and Figs. 3 and 4 show that the TVD-Hopmoc

method in conjunction with the Monotonized Central scheme [25] obtained in general better results than employing the other four flux-limiter schemes. On the other hand, Koren's scheme [26] achieved better results than the other schemes when employed in simulations with $\frac{\Delta t}{\Delta x} = 0.8$. Moreover, Tables 2 and 3 and Fig. 5 show that the TVD-Hopmoc method (along with the Monotonized Central scheme [25]) obtains better accuracy results than the Hopmoc method using an interpolation technique.

Table 3. Maximum errors when setting $\Delta x = 0.001$ and Reynolds number (Re) established as 2000 and 3000 in simulations employing the TVD-Hopmoc along with five flux-limiter formulations and the Hopmoc method with and without (w/o) using a linear interpolation (int.). The symbol \dagger indicates that the convergence was not achieved

Re	Δt	$\frac{\Delta t}{\Delta x}$	Hopmoc		TVD-Hopmoc				
			w/o int.	int.	V. Leer	MinMod	Superbee	MC	Koren
2000	$2.00 \cdot 10^{-4}$	0.20	0.0000	3.1551	0.0142	0.0902	0.0852	0.0139	0.0362
	$2.50 \cdot 10^{-4}$	0.25	0.0000	2.9897	0.0111	0.0845	0.0800	0.0109	0.0318
	$31.25 \cdot 10^{-5}$	0.31	0.0000	2.7781	0.0077	0.0775	0.0733	0.0075	0.0267
	$4.00 \cdot 10^{-4}$	0.40	0.0000	2.4721	0.0058	0.0676	0.0639	0.0035	0.0203
	$5.00 \cdot 10^{-4}$	0.50	0.0000	2.1075	0.0051	0.0566	0.0526	0.0015	0.0140
	$6.25 \cdot 10^{-4}$	0.63	0.0000	1.6279	0.0040	0.0427	0.0389	0.0028	0.0078
	$8.00 \cdot 10^{-4}$	0.80	0.0000	0.9066	0.0036	0.0223	0.0197	0.0037	0.0023
	$1.00 \cdot 10^{-3}$	1.00	0.0000	0.0008	\dagger				
	$1.25 \cdot 10^{-3}$	1.25	0.0000	0.6906					
	$156.25 \cdot 10^{-5}$	1.56	0.0000	0.7272					
	$2.00 \cdot 10^{-3}$	2.00	0.0000	0.0187					
	$2.50 \cdot 10^{-3}$	2.50	0.0001	0.4776					
	$31.25 \cdot 10^{-4}$	3.13	0.0001	0.1717					
	$4.00 \cdot 10^{-3}$	4.00	0.0003	0.0803					
	$6.25 \cdot 10^{-3}$	6.25	0.0007	0.2373					
	$1.00 \cdot 10^{-2}$	10.00	0.0019	1.2599					
3000	$2.00 \cdot 10^{-4}$	0.2	0.0000	4.5060	0.0248	0.1584	0.1441	0.0239	0.0620
	$2.50 \cdot 10^{-4}$	0.25	0.0000	4.2807	0.0195	0.1484	0.1350	0.0187	0.0545
	$31.25 \cdot 10^{-5}$	0.31	0.0000	3.9905	0.0142	0.1360	0.1242	0.0129	0.0457
	$4.00 \cdot 10^{-4}$	0.40	0.0000	3.5678	0.0123	0.1187	0.1086	0.0060	0.0347
	$5.00 \cdot 10^{-4}$	0.50	0.0000	3.0590	0.0103	0.0987	0.0907	0.0030	0.0240
	$6.25 \cdot 10^{-4}$	0.63	0.0000	2.3807	0.0073	0.0738	0.0685	0.0047	0.0133
	$8.00 \cdot 10^{-4}$	0.80	0.0000	1.3410	0.0063	0.0386	0.0365	0.0061	0.0036
	$1.00 \cdot 10^{-3}$	1.00	0.0000	0.0001	\dagger				
	$1.25 \cdot 10^{-3}$	1.25	0.0000	1.0236					
	$156.25 \cdot 10^{-5}$	1.56	0.0000	1.0742					
	$2.00 \cdot 10^{-3}$	2.00	0.0000	0.0097					
	$2.50 \cdot 10^{-3}$	2.50	0.0001	0.7015					
	$31.25 \cdot 10^{-4}$	3.13	0.0001	0.2535					
	$4.00 \cdot 10^{-3}$	4.00	0.0002	0.0457					
	$5.00 \cdot 10^{-3}$	5.00	0.0003	0.0230					
	$6.25 \cdot 10^{-3}$	6.25	0.0005	0.2788					
	$1.00 \cdot 10^{-2}$	10.00	0.0015	0.3011					

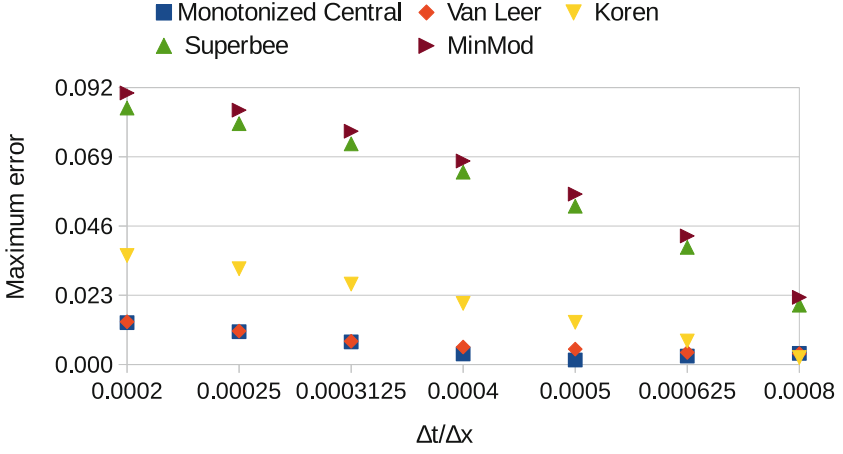


Fig. 3. Maximum errors when setting $\Delta x = 0.001$ and Reynolds number (Re) established as 2000 in simulations employing the TVD–Hopmoc method alongside five flux–limiter formulations

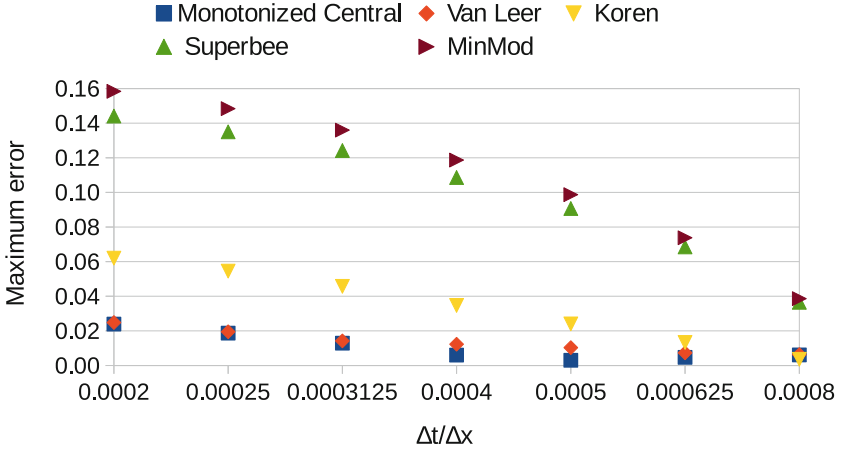


Fig. 4. Maximum errors when setting $\Delta x = 0.001$ and Reynolds number (Re) established as 3000 in simulations employing the TVD–Hopmoc method alongside five flux–limiter formulations

The Hopmoc method is independent of the CFL condition. On the other hand, the TVD–Hopmoc method does not converge for $v \cdot \frac{\Delta t}{\Delta x} \geq 1$ because it is based on the Lax–Wendroff method that was used to obtain the Total Variation Diminishing formulation.

When the foot of the characteristic line is a nodal point (i.e. a very particular case), Tables 2 and 3 show that the results obtained when applying the original Hopmoc method without linear interpolation is better than using Total Variation Diminishing schemes. However, for instance when the velocity field is

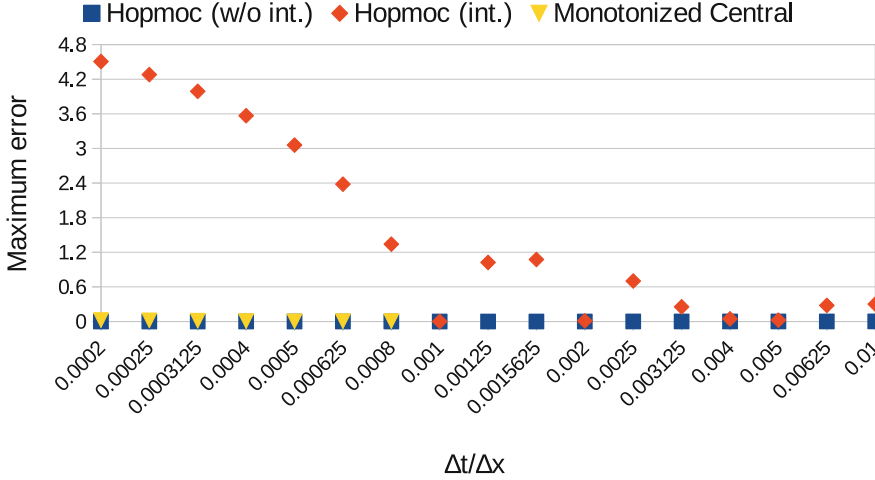


Fig. 5. Maximum errors when setting $\Delta x = 0.001$ and Reynolds number (Re) established as 3000 in simulations employing the Hopmoc and TVD–Hopmoc methods alongside the Monotonized Central scheme [25]

non-uniform, this peculiar circumstance (i.e. the foot of the characteristic line as a nodal point) does not occur.

5 Conclusions and Future Works

This work presented the Hopmoc method along with a Total Variation Diminishing scheme (TVD–Hopmoc for short) for the solution of parabolic equations with convective dominance without solving linear systems. The TVD–Hopmoc method computes previous values by tracking them along characteristic lines and employs a flux–limiter formulation to provide higher precision solutions than the original Hopmoc method. This work compared five flux–limiter formulations along with the Hopmoc method. The Monotonized Central scheme [25] yielded in general better results than the other four schemes in simulations with three Reynolds number regimes. On the other hand, Koren’s scheme [26] delivered better results than the other schemes in simulations with $\frac{\Delta t}{\Delta x} = 0.8$ (see Tables 2 and 3). Thus, this paper provided numerical experiments that show the advantages of the new approach compared with the original Hopmoc method. Specifically, the numerical results obtained with the new TVD–Hopmoc strategy provided effective improvements over the original Hopmoc method for simulations with Courant number smaller than 1 since the flux–limiter formulations employed here are based on the Lax–Wendroff method.

Naturally, the Hopmoc method is more accurate when values from previous time steps are obtained from nodal points when tracking them along the characteristic line. However, this situation is a very particular case for a uniform

velocity field so that more experiments are necessary to be carried out in the case of non-uniform velocity fields.

Furthermore, the Total Variation Diminishing property does not guarantee that one extrema grows whereas another nearby extrema diminishes [19]. Then, other approaches using positive schemes and universal limiters will be evaluated in future studies. In addition, we intend to evaluate those schemes when applying them to 2-D and 3-D parallel cases so that the scalability of this approach will be also evaluated in future investigations. Additionally, we plan to compare how well the proposed new method performs compared with other approaches, especially one based on an approach of solving systems of linear algebraic equations.

References

1. Cabral, F.L., Osthoff, C., Costa, G., Brandão, D.N., Kischinhevsky, M., Gonzaga de Oliveira, S.L.: Tuning up TVD HOPMOC method on Intel MIC Xeon Phi architectures with Intel Parallel Studio tools. In: 2017 29th International Symposium on Computer Architecture and High Performance Computing Workshops (SBAC-PADW), Campinas, pp. 19–24 (2017). <https://ieeexplore.ieee.org/document/8109000/>
2. Ding, H., Zhang, Y.: A new difference scheme with high accuracy and absolute stability for solving convection-diffusion equations. *J. Comput. Appl. Math.* **230**, 600–606 (2009)
3. Holstad, A.: The Koren upwind scheme for variable gridsize. *Appl. Numer. Math.* **37**, 459–487 (2001)
4. Kischinhevsky, M.: An operator splitting for optimal message-passing computation of parabolic equation with hyperbolic dominance. In: SIAM Annual Meeting, Kansas City, MO (1996)
5. Kischinhevsky, M.: A spatially decoupled alternating direction procedure for convection-diffusion equations. In: Proceedings of the XXth CILAMCE Iberian Latin American Congress on Numerical Methods in Engineering (1999)
6. Gane, C.R., Gourlay, A.R.: Block hopscotch procedures for second order parabolic differential equations. *J. Inst. Math. Appl.* **19**, 205–216 (1977)
7. Gordon, P.: Nonsymmetric difference equations. *SIAM J. Appl. Math.* **13**, 667–673 (1965)
8. Gourlay, A.R.: Hopscotch: a fast second order partial differential equation solver. *IMA J. Appl. Math.* **6**, 375–390 (1970)
9. Gourlay, A.R., McGuire, G.R.: General Hopscotch algorithm for the numerical solution of partial differential equations. *J. Inst. Math. Appl.* **7**, 216–227 (1971)
10. Gourlay, A.R., McKee, S.: The construction of Hopscotch methods for parabolic and elliptic equations in two space dimensions with mixed derivative. *J. Comput. Appl. Math.* **3**, 201–206 (1977)
11. Douglas Jr., J., Russel, T.F.: Numerical methods for convection-dominated diffusion problems based on combining the method of characteristics with finite element or finite difference procedures. *SIAM J. Numer. Anal.* **19**, 871–885 (1982)
12. Celia, M.A., Russel, T.F., Herrera, I., Ewing, R.E.: An Eulerian-Lagrangian localized adjoint method for the advection-diffusion equation. *Adv. Water Resour.* **13**, 187–206 (1990)
13. Russel, T.F., Celia, M.A.: An overview of research on Eulerian-Lagrangian localized adjoint methods (ELLAM). *Adv. Water Resour.* **25**, 1215–1231 (2002)

14. Cabral, F.L., Osthoff, C., Kischinhevsky, M., Brandão, D.: Hybrid MPI/OpenMP/OpenACC implementations for the solution of convection diffusion equations with Hopmoc method. In: Aduhan, B., Rocha, A.M., Misra, S., Taniar, D., Gervasi, O., Murgante, B. (eds.): 14th International Conference on Computational Science and its Applications (ICCSA) CPS, 196–199. IEEE, July 2014
15. Harten, A.: High resolution schemes for hyperbolic conservation laws. *J. Comput. Phys.* **49**, 357–393 (1983)
16. Bartels, S., Nochetto, R.H., Salgado, A.J.: A total variation diminishing interpolation operator and applications. *Math. Comput.* **84**, 2569–2587 (2015)
17. Fernandes, B.R.B., Gonçalves, A.D.R., Filho, E.P.D., Lima, I.C.M., Marcondes, F., Sepehrnouri, K.: A 3D total variation diminishing scheme for compositional reservoir simulation using the element-based finite-volume method. *Numer. Heat Transfer, Part A* **67**(8), 839–856 (2015)
18. Oliveira, S.R.F., Gonzaga de Oliveira, S.L., Kischinhevsky, M.: Convergence analysis of the Hopmoc method. *Int. J. Comput. Math.* **86**, 1375–1393 (2009)
19. Thuburn, J.: TVD schemes, positive schemes and universal limiter. *Mon. Weather Rev.* **125**, 1990–1993 (1997)
20. Courant, R., Isaacson, E., Rees, M.: On the solution of nonlinear hyperbolic differential equations by finite differences. *Commun. Pure Appl. Math.* **5**(3), 243–255 (1952)
21. Waterson, N.P., Deconinck, H.: Design principles for bounded higher-order convection schemes - a unified approach. *J. Comput. Phys.* **224**, 182–207 (2007)
22. Sweby, P.K.: High resolution schemes using flux limiters for hyperbolic conservation laws. *SIAM J. Numer. Anal.* **21**(5), 995–1011 (1984)
23. Roe, P.L., Baines, M.J.: Algorithms for advection and shock problems. In: Viviand, H. (ed.): *Proceedings of the Fourth GAMM Conference on Numerical Methods in Fluid Mechanics. Notes on Numerical Fluid Mechanics*, vol. 5, pp. 281–290. Vieweg, Paris, France (1982)
24. Roe, P.L.: Some contributions to the modelling of discontinuous flows. In: Engquist, B.E., Osher, S., Somerville, R.C.J. (eds.): *Proceedings of the Fifteenth Summer Seminar on Applied Mathematics Large-Scale Computations in Fluid Mechanics. Lectures in Applied Mathematics*, vol. 22, pp. 163–193. AMS-SIAM Summer Seminar, American Mathematical Society, La Jolla, CA (1985)
25. van Leer, B.: Towards the ultimate conservative difference schemes. *J. Comput. Phys.* **14**, 361–370 (1974)
26. Koren, B.: A robust upwind discretization method for advection, diffusion and source terms. In: Vreugdenhil, C.B., Koren, B. (eds.) *Numerical Methods for Advection - Diffusion Problems. Notes on Numerical Fluid Mechanics*, vol. 45, pp. 117–138. Friedrich Vieweg & Sohn Verlagsgesellschaft, Braunschweig, Germany, October 1993